First β-delayed neutron spectroscopy of ^{24}O

S. Neupane,[1,2,*] N. Kitamura,[1,3] Z. Y. Xu,[1] R. Grzywacz,[1,4] S. J. Novario,[5] J. Okołowicz,[6,7] M. Płoszajczak,[7] B. S. Hu,[8,4] J. M. Allmond,[4] A. Chester,[9] J. M. Christie,[1] I. Cox,[1] J. Farr,[1] I. Fletcher,[1] J. Heideman,[1] D. Hoskins,[1] T. T. King,[1] A. Laminack,[4] S. N. Liddick,[9,10] M. Madurga,[1] A. L. Richard,[9] P. Shuai,[1,4] K. Siegl,[1] P. Wagenknecht,[4] and R. Yokoyama[1]

[1]*Department of Physics and Astronomy, University of Tennessee, Knoxville, Tennessee 37996, USA*
[2]*Lawrence Livermore National Laboratory, Livermore, California 94551, USA*
[3]*Center for Nuclear Study, University of Tokyo, Wako, Saitama 351-0198, Japan*
[4]*Physics Division, Oak Ridge National Laboratory, Oak Ridge, Tennessee 37831, USA*
[5]*Los Alamos National Laboratory, Los Alamos, New Mexico 87545, USA*
[6]*Institute of Nuclear Physics, Polish Academy of Sciences, Radzikowskiego 152, PL-31342 Kraków, Poland*
[7]*Grand Accélérateur National d'Ions Lourds (GANIL), CEA/DSM - CNRS/IN2P3, BP 55027, F-14076 Caen Cedex, France*
[8]*National Center for Computational Sciences, Oak Ridge National Laboratory, Oak Ridge, Tennessee 37831, USA*
[9]*Facility for Rare Isotope Beams, Michigan State University, East Lansing, Michigan 48824, USA*
[10]*Department of Chemistry, Michigan State University, East Lansing, Michigan 48824, USA*

(Dated: September 10, 2024)

The β decay of ^{24}O was investigated at NSCL/MSU using a combination of neutron and γ-ray spectroscopy. For the first time, the β-delayed neutron energy spectrum of ^{24}O was measured, revealing three intensely populated, isolated neutron-unbound states in ^{24}F. This allowed for the extraction of the decay strength in ^{24}F up to 6.2 MeV. A comprehensive comparison of the experimental results with various nuclear theories was conducted, ranging from the empirical shell model to the most advanced ab initio calculations. While most theoretical predictions align with the experimental data for low-lying states, discrepancies arise at higher excitation energies. In the transition from ^{24}O to ^{24}F, shell model calculations using the empirical USDB interaction predicted the structure of both nuclei without invoking the need for a stronger proton-neutron tensor force, which was postulated for the neighboring isotone ^{25}F.

Introduction— Large proton-neutron asymmetry plays a pivotal role in altering the nuclear structure of unstable nuclei compared with their stable counterparts. Therefore, one of the prime focuses of the next generation of radioactive ion beam facilities is to characterize the structure evolution of the short-lived isotopes moving away from stability. Recent experimental efforts have revealed new phenomena in those exotic nuclei, such as the disappearance of conventional magic numbers and the emergence of new magic numbers [1, 2]. Another example is the peculiar behavior of the limits of nuclear binding. The neutron drip line in carbon ($Z = 6$), nitrogen ($Z = 7$), and oxygen ($Z = 8$) is experimentally known to be at $N = 16$. However, it rapidly extends to $N = 22$ for fluorine ($Z = 9$), and this sudden jump is referred to as the oxygen drip-line anomaly [3]. Furthermore, recent work by Tang *et al.* [4] indicated that the core of ^{25}F, a nucleus that is one proton away from ^{24}O, is significantly differs from the ^{24}O ground state. As such, neutron-rich oxygen and fluorine isotopes are expected to provide a critical benchmark to study the effects of the spin-isospin dependent interaction, three-body forces, and the coupling to the continuum, which, in turn, determine the location of the neutron drip line [5, 6]. While ^{24}O is known to be the last bound isotope of the $Z = 8$ isotopic chain [3], a wealth of recent measurements indicated a spherical $N = 16$ shell closure originating from the large spin-orbit splitting between the neutron $d_{3/2}$ and $d_{5/2}$ orbitals [7–10]. Consequently, ^{24}O is established as a doubly-magic drip-line nucleus. The recent observation of the ^{28}O resonance, which decays to ^{24}O via four neutron emission, also emphasized the doubly-magic nature of ^{24}O [11].

The β decay of neutron-rich oxygen isotopes probes the transition to the corresponding fluorine isotopes. In particular, the decay of ^{24}O is expected to be simple; to first order, the allowed Gamow-Teller (GT) transitions can be described by transforming either a $d_{5/2}$ neutron to a $d_{5/2}$ proton, or a $s_{1/2}$ neutron to a $s_{1/2}$ proton. As a result, 1^+ states in ^{24}F with relatively pure configurations are populated, owing to the selectivity of the GT transition. Hence, decay studies of ^{24}O are uniquely suited to test nuclear models that aim to describe the nuclear structure approaching the neutron drip line and beyond. Due to the large β-decay Q-value (Q_β) of 10.97(19) MeV [12], the β decay of ^{24}O populates both bound and unbound states in ^{24}F, the latter lying above its neutron separation energy of 3.81(10) MeV [12], thus allowing for the β-delayed neutron emission. Neutron spectroscopy provides unique access to the neutron unbound states in the daughter, which are otherwise difficult to study by other means.

The β decay of ^{24}O was first studied by Mueller *et al.* [13], and they reported a half-life of 61^{+31}_{-19} ms and a neutron branching ratio of 58(12) %. A similar measure-

* neupane1@llnl.gov

ment, performed by Reed *et al.* [14], reported a half-life of 65(5) ms, which agrees within the uncertainty given in the earlier measurement, but indicated a significantly lower neutron branching ratio of 18(6) %. Later, Penionzhkevich *et al.* [15] reported a similar half-life of 67(10) ms and a neutron branching ratio of 12(8) %. However, the most recent measurement performed by Cáceres *et al.* [16] presented a slightly longer half-life of 80(5) ms and again a higher neutron branching ratio of 43(4) %.

The bound excited states at 521.5(3) and 1831.6(5) keV in ^{24}F were first identified by Reed *et al.* [14] and this result was confirmed by Cáceres *et al.* [16]. Furthermore, Cáceres *et al.* performed a complementary measurement using in-beam γ-ray spectroscopy, and new excited states in ^{24}F at 2384(64), 2739(14), 3639(22), and 3562(42) keV were proposed. However, states above the neutron threshold (S_n) have not yet been explored. By employing both γ-ray and neutron spectroscopy, we extend our knowledge of ^{24}F above S_n, providing more complete nuclear structure information of this neutron-rich isotope next to ^{24}O.

Experiment— In this Letter, we report on the first β-delayed neutron spectroscopy of ^{24}O. The experiment was performed at the National Superconducting Cyclotron Laboratory at Michigan State University. A primary beam of ^{48}Ca was accelerated to a kinetic energy of 140 MeV/nucleon using the Couple Cyclotron Facility [17] and directed onto an 846-mg/cm^2 thick beryllium target, producing a secondary cocktail beam by projectile fragmentation. The isotopes of interest were separated from all other reaction products and guided to the experimental area using the A1900 fragment separator [18]. The isotopes were identified on an event-by-event basis by measuring the time-of-flight between a plastic scintillator in the A1900 focal plane and a silicon PIN detector upstream of the experimental setup, as well as the energy loss in the PIN detector. In this separator setting, nuclei spanning from boron to aluminum near the neutron drip line were produced. The implantation rate for ^{24}O was approximately 6 particles per second, with a beam purity of around 1.1%.

The experimental setup includes a scintillator array for neutrons and germanium clovers for γ rays. At the heart of the setup is an implantation detector for identifying ion implantation and their subsequent β-decay events, which comprised of a 12 mm thick Yttrium Orthosilicate (YSO) detector [19], with an active surface area of 48×48 mm^2 and 24×24 pixels, allowing for the recording of energy and timing information of ion implantation and β-decay events for the ion implantation and corresponding decay event correlation.

The Versatile Array of Neutron Detectors at Low Energy (VANDLE) [20, 21] was used for the time-of-flight (TOF) measurements of β-delayed neutrons. A full array consisting of 48 plastic scintillator bars, resulting in a total neutron detection efficiency of 11% at 1 MeV, was placed at a distance of 105 cm measured between the center of the implantation detector and the front face of the bar. Three high-purity germanium clovers from the CLARION array [22] were installed on the other side of the setup for γ-ray detection. These detectors provided a total photopeak efficiency of 1.3% at 1 MeV.

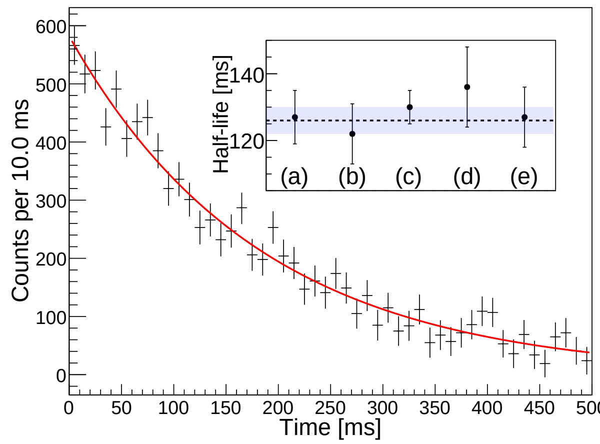

FIG. 1: Background-subtracted decay curve obtained by summing the gates on 521, 1309, 1830 keV γ-ray transitions in ^{24}F following the decay of ^{24}O. A half-life of 126(4) ms was obtained from the fit (red solid line). Inset shows the half-life extracted using different gating methods: (a) 521 keV γ ray, (b) 1309 keV γ ray, (c) 1830 keV γ ray, (d) neutrons, and (e) no gates. The half-life reported in this work is shown as the black dotted line with the light blue band.

Analysis and Results— Ion-β correlation was performed using the ^{24}O implantation and β-decay events measured in the YSO detector based on their spatial and timing information. In the present analysis, a radius of 0.35 cm was used. The optimal correlation radius was determined to retain a high signal-to-background ratio [19]. A background-subtracted γ-ray gated decay curve with a correlation time window of $\pm$500 ms is shown in Fig. 1. This decay curve was obtained by summing the individual contributions from observed γ-ray transitions in ^{24}F following the decay of ^{24}O as shown in Fig. 2. The events contained within the negative correlation time were used to model the background originating from random β signals associated with each implant. The negative correlation part of the decay curve is flipped around the time zero and then subtracted on a bin-by-bin basis to obtain a background-subtracted decay curve. A single exponential fit yielded a half-life of 126(4) ms for the ^{24}O decay, which is significantly longer than the literature value of 72(5) ms [23]. We also extracted half-lives using different gating methods: gating on individual γ-ray transitions, neutrons, and without any gates applied. The half-lives agree with each other within uncertainties, as shown in the inset of Fig. 1.

The β-delayed γ-ray spectrum of ^{24}O, with add-back enabled, is shown in Fig. 2. An ion-β correlation window of $\pm$500 ms was chosen for optimized spectral quality. The background spectrum was obtained by gating on events in the negative time window (before ion implantation) of the decay curve. The correlated spectrum was

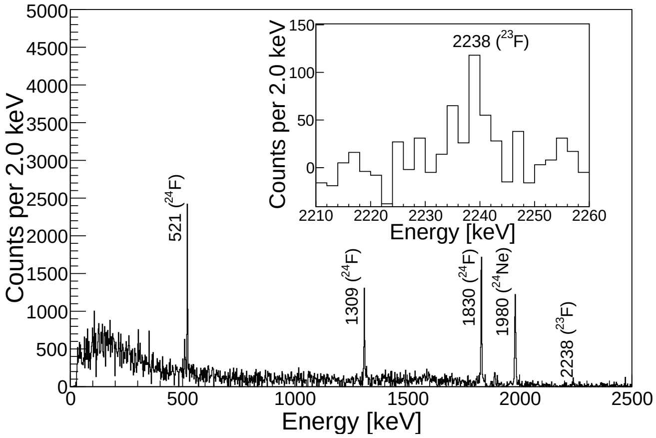

FIG. 2: Background-subtracted add-back γ-ray spectrum following the decay of ^{24}O occurring within 500 ms after implantation. The inset shows the spectrum zoomed around the 2238(4) keV γ ray.

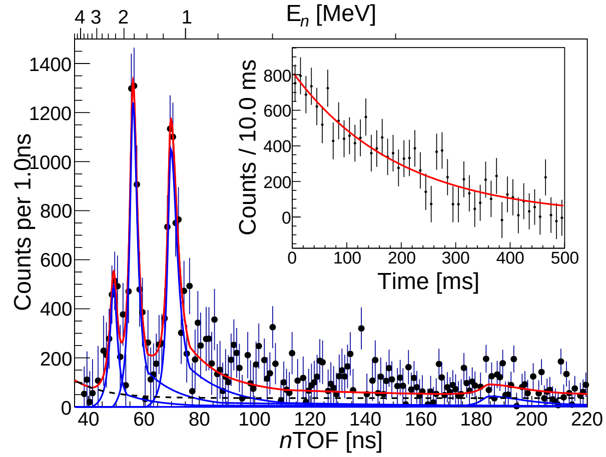

FIG. 3: Neutron singles TOF spectrum (black points) along with the analytical fitting function (red). The contribution from individual peaks is shown in blue, and the black dashed line represents the continuous background. The inset shows the neutron-gated decay curve.

then obtained by subtracting the background spectrum from the spectrum gated on the positive time window (after ion implantation) of the decay curve on a bin-by-bin basis. The same approach was used for the neutron TOF analysis. The γ-ray peaks at 521(1), 1309(1), and 1830(2) keV, as reported in the previous β-γ measurements [14, 16], were clearly identified in the present spectrum. These are attributed to two bound excited states in ^{24}F. From the γ-γ coincidence analysis, it was confirmed that the state at 1830 keV is predominantly populated in the β decay, and it deexcites by emitting a 1830 keV γ ray or via a cascade of 1309 and 521 keV γ rays. An intensity balance consideration placed the 1309 keV transition on top of the 521 keV γ ray. The present measurement also confirms the very weak direct population of the 521 keV state, and this is in line with the 2^+ assignment discussed in the previous works, as well as the ground-state spin-parity of 3^+, made based on comparisons with shell-model calculations (see Refs. [14, 16] for details).

Figure 3 presents the background-subtracted β-delayed neutron TOF spectrum obtained for the ^{24}O decay within a correlation time window of $\pm$500 ms. Three well-separated neutron peaks, with energies ranging from 1.2 to 2.4 MeV, were observed in this spectrum. Since two-neutron emission is energetically prohibited (S_{2n} = 11.39(10) MeV in ^{24}F is greater than Q_β = 10.97(19) MeV of ^{24}O [12]), one-neutron emission from ^{24}F is the sole contributor to the spectrum. To determine the energies of the neutron peaks and their number of counts, the neutron TOF spectrum was fitted with a combination of template detector response functions and an exponential background. The response functions were generated by Geant4 [24, 25] simulations that use the exact geometry of the detector system and validated by the three well-established, prominent neutron lines of β-delayed neutron emission from ^{17}N [26]. The fitting procedure is described in detail in Ref. [27]. The best

TABLE I: β-feeding intensities (I_β) and logft values for the GT states, and intensities of observed γ-ray transitions (I_γ) in ^{24}F. The states are labeled by their excitation energies (E_x) measured from the ground state.

E_x (keV)	I_β (%)	E_γ (keV)	I_γ (%)	logft
521(1)	-	521(1)	20(2)	-
1830(2)	62(11)	1830(2)	41(4)	4.3(1)
		1309(1)	19(2)	
5031(22)	11(2)	-	-	4.2(1)
5684(37)	11(2)	-	-	3.9(1)
6223(51)	8(2)	-	-	3.8(1)

fit is displayed in Fig. 3, and as tabulated in Table I, the level energies of neutron unbound states in ^{24}F were reconstructed by summing the energy carried by neutron emission after correcting for recoil effects and the neutron separation energy. The number of counts under each neutron peak was obtained from the fit and corrected using the energy-dependent efficiency curve to get the total number of neutrons feeding to the excited and ground states of ^{23}F. By normalizing the total number of neutrons feeding the excited and ground states of ^{23}F to the total number of β decays (N_β), a β-delayed neutron branching ratio of 30(5)% was obtained.

The three major neutron lines likely correspond to transitions that feed the ^{23}F ground state, considering their intensities. We note that, in the γ-ray analysis, the first excited state in ^{23}F was found to be populated with a weak feeding (see the inset of Fig. 2). We observed the same state populated in ^{23}F from the decay of ^{23}O in the present measurement. A neutron-γ ray cascade originating from the 6223 keV state in ^{24}F would produce a neutron with a kinetic energy of around 170 keV, as depicted schematically in Fig. 4. The neutron spectrum hints at a small peak at $\sim$185 ns; however, identifying such a neutron branch is challenging because of the lim-

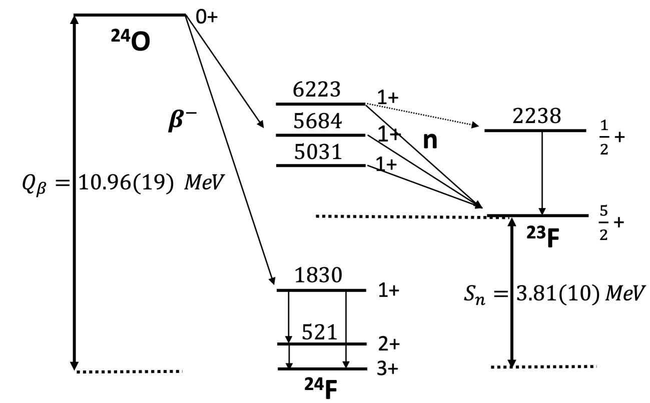

FIG. 4: Schematic illustration of the decay scheme of ^{24}O observed in the present experiment. Note that the vertical axis is not to scale, and level energies are in keV. The spin and parities of the bound states are adopted from Ref. [23, 28].

ited statistics and the detection threshold in the present experiment, and it awaits future experimental verification. Table I also summarizes β-feeding intensities (I_β) for each state and intensities of observed γ rays (I_γ) in ^{24}F obtained by normalizing the individual intensities to N_β. It is noted that the contribution from feeding to the 2238 keV state in ^{23}F was taken into account while calculating I_β for the 6223 keV state in ^{24}F. Logft values were calculated using the half-life, excitation energies, and branching ratios from the present work, along with Q_β from Ref. [12]. The logft values for the bound 1830 keV state and three neutron unbound states were found to span from 3.8 to 4.3. This favors GT transitions, leading to spin-parity assignments of 1^+ to these states.

Comparision with nuclear model calculations— Based on the experimental logft values, the GT transition strengths, B(GT), extending to neutron unbound states in ^{24}F, were deduced for the first time. The experimental level energies and strength distribution were then compared with predictions made by various nuclear models. To begin with, we performed shell-model calculations with the USDB effective interaction [29]. This empirical shell-model interaction, constructed within the *sd*-shell model space, has been shown to give reliable predictions of nuclear properties in this mass region. To benchmark ab initio nuclear models, calculations were performed using two different approaches, the valence space in-medium similarity renormalization group (VS-IMSRG) [30, 31] and the coupled-cluster (CCSDT-3) [32] method. In the VS-IMSRG calculations, the Hamiltonian was derived using the 1.8/2.0 (EM) interaction [33] and diagonalized in the *sd*-shell model space. In the CCSDT-3 calculations, the same 1.8/2.0 (EM) interaction was used, but the diagonalization was performed using the equation-of-motion method [34]. Effects arising from two-body currents [35] were taken into account when calculating B(GT) in both VS-IMSRG and CCSDT-3. To study the roles played by the coupling to the continuum, level energies and B(GT) were calculated using the shell model embedded in the continuum (SMEC) approach [36] with the monopole adjusted WBP− interaction [37], supplemented by the Wigner-Bartlett continuum-coupling interaction [38]. The results of these theoretical predictions are displayed in Fig. 5, together with the experimental values.

All calculations consistently reproduce the bound-state structure of ^{24}F. Guided by these results, the spin-parity of the ground (first-excited) state is highly likely 3^+ (2^+). The location of the first 1^+ state and its GT strength are in good agreement with the predictions by these models. However, discrepancies become more pronounced above the neutron threshold. As such, the unbound 1^+ states provide a critical testing ground for different theoretical models. The USDB calculations predict the location of the unbound states remarkably well, although the GT strengths to these states tend to be underestimated. The ab initio calculations, VS-IMSRG and CCSDT-3, show more concentrated strength distributions, which differ from the experimental observation. One should note that USDB and VS-IMSRG predicted a 1^+ state near the neutron separation energy with a small GT strength. The non-observation of this state in the experiment can be attributed to the small β feeding. A low detection efficiency for high-energy γ rays or the lack of sensitivity to low-energy neutrons would provide an additional explanation.

Discussion— The USDB shell-model interaction is constructed relying on fit to experimental data, thus making it an empirical model. During the fitting process, evolving shell structures originating from spin-isospin-dependent terms of NN interactions, as well as three-body effects, are implicitly taken into account. It is generally considered that this interaction is capable of predicting properties of *sd*-shell nuclei, including unstable ones, apart from those near the $N = 20$ island of inversion, where the fp-shell degree of freedom plays a significant role.

Recently, this was questioned by Tang *et al.* [4]. According to this experimental work, a significant modification to the USDB interaction, specifically, 3−4 MeV reduction in the $\nu d_{3/2}$ single particle energy (SPE), was required to reproduce the experimental data on one-proton removal from ^{25}F that produces ^{24}O final states. This implies that a much stronger proton-neutron tensor force than that implemented in the original USDB is needed, and it was proposed that such a constituent may be responsible for the oxygen dripline anomaly. However, our finding indicates that such a change is not compatible with the present experimental result, as evident in Fig. 6. Reducing the $\nu d_{3/2}$ SPE in ^{24}F by 3 MeV resulted in a more pronounced disagreement of the predicted excitation energies and strength distribution with the experiment. The quenched shell gap notably fails to predict the position of the first 1^+ state in ^{24}F, signifying that the strong proton-neutron tensor force is not necessary

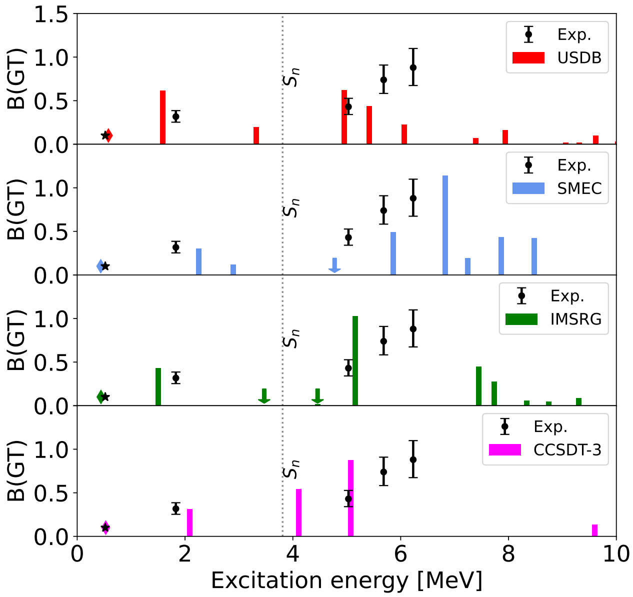

FIG. 5: GT transition strengths, B(GT), associated with the observed 1^+ states in ^{24}F (black points), in comparison with various nuclear model calculations, Shell-model results using the empirical USDB interaction (first panel), predictions from the shell model embedded in the continuum (SMEC, second panel), and ab initio calculations using the valence space in-medium similarity renormalization group (VS-IMSRG, third panel) and the coupled-cluster method (CCSDT-3, fourth panel). The diamonds (star) represent the location of the theoretical (experimental) 2^+ states, and the down arrows point to the location of other 1^+ states around S_n with very small B(GT).

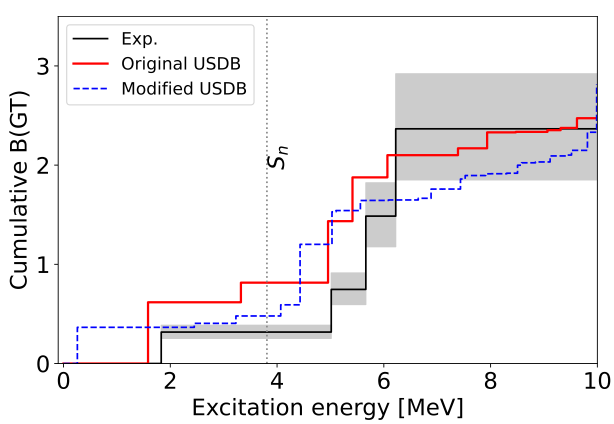

FIG. 6: Cumulative B(GT) predictions using the USDB interaction with the $\nu d_{3/2}$ single particle energy in ^{24}F reduced by 3 MeV (blue dashed) compared to the original value of 2.11 MeV (red solid) and the experiment (black solid).

to describe these nuclei. The ^{24}O results obtained in the present work are in stark contrast with the conclusions in Ref. [4] for the $N = 16$ nucleus ^{25}F.

Furthermore, to address discrepancies between effective and ab initio calculations, we analyzed the wave functions from both USDB and VS-IMSRG. For the first 1^+ state of ^{24}F, the two approaches yield similar occupation numbers for proton and neutron orbitals. However, in the neutron-unbound 1^+ states with large B(GT) values, VS-IMSRG predicts that the proton predominantly occupies the $d_{5/2}$ orbital, while USDB shows a more fragmented distribution among the proton $d_{5/2}$, $s_{1/2}$, and $d_{3/2}$ orbitals. The agreement with experimental data suggests that, despite being phenomenological and data-fitted, USDB includes the necessary interactions to induce correlations in the proton wave functions in these highly excited states. On the other hand, incorporating these strong collective correlations and/or continuum coupling effects into ab initio calculations at high excitation energies remains a significant challenge for future development.

Conclusion— We have reported the first β-delayed neutron spectroscopy of ^{24}O. Combining γ-ray and neutron TOF measurements, we extracted β-decay strengths extending to the neutron unbound states in ^{24}F. The new experimental data allowed for comparisons with various theoretical calculations. Shell-model calculations using the standard USDB interaction produced a fairly good overall agreement with the measurement, suggesting that the transition from ^{24}O to ^{24}F can be described without invoking dramatic changes to the shell structure, such as the implementation of a much stronger proton-neutron tensor force. The present data has provided important tests of ab initio calculations using the VS-IMSRG and coupled-cluster approaches. These calculations reproduce well the structure of ^{24}F around its ground state. However, disagreements are more pronounced for the neutron unbound states. This implies that predicting the decay properties of the neutron-rich nucleus is not trivial, and optimizations are still required. A more complete description of the experimental finding and a better understanding of the underlying effects of nuclear structure await further theoretical developments.

ACKNOWLEDGMENTS

This research was partly sponsored by the National Nuclear Security Administration under the Stewardship Science Academic Alliances program through DOE Cooperative Agreements No. DE-NA0003899 and DE-NA0004068. This material is based upon work supported in part by the U.S. Department of Energy, Office of Science, Office of Nuclear Physics under Contract No. DE-FG02-96ER40983 (UTK), DE-SC0020451 (MSU), and DE-AC05-00OR22725 (ORNL). This research was sponsored in part by the National Science Foundation under the contract NSF-MRI-1919735. This work was also supported by the National Nuclear Security Administration through the Nuclear Science and Security Consortium under Award No. DE-NA0003180 and the Stewardship Science Academic Alliances program through DOE Award No. DOE-DE-NA0003906.

[1] T. Otsuka, A. Gade, O. Sorlin, T. Suzuki, and Y. Utsuno, Reviews of Modern Physics **92**, 015002 (2020).

[2] O. Sorlin and M.-G. Porquet, Progress in Particle and Nuclear Physics **61**, 602 (2008).

[3] Y. Kondo, T. Nakamura, R. Tanaka, R. Minakata, S. Ogoshi, N. Orr, N. Achouri, T. Aumann, H. Baba, F. Delaunay, *et al.*, Physical Review Letters **116**, 102503 (2016).

[4] T. L. Tang, T. Uesaka, S. Kawase, D. Beaumel, M. Dozono, T. Fujii, N. Fukuda, T. Fukunaga, A. Galindo-Uribarri, S. H. Hwang, N. Inabe, D. Kameda, T. Kawahara, W. Kim, K. Kisamori, M. Kobayashi, T. Kubo, Y. Kubota, K. Kusaka, C. S. Lee, Y. Maeda, H. Matsubara, S. Michimasa, H. Miya, T. Noro, A. Obertelli, K. Ogata, S. Ota, E. Padilla-Rodal, S. Sakaguchi, H. Sakai, M. Sasano, S. Shimoura, S. S. Stepanyan, H. Suzuki, M. Takaki, H. Takeda, H. Tokieda, T. Wakasa, T. Wakui, K. Yako, Y. Yanagisawa, J. Yasuda, R. Yokoyama, K. Yoshida, K. Yoshida, and J. Zenihiro, Physical Review Letters **124**, 212502 (2020).

[5] T. Otsuka, T. Suzuki, J. D. Holt, A. Schwenk, and Y. Akaishi, Physical Review Letters **105**, 032501 (2010).

[6] G. Hagen, M. Hjorth-Jensen, G. Jansen, R. Machleidt, and T. Papenbrock, Physical Review Letters **108**, 242501 (2012).

[7] A. Ozawa, T. Kobayashi, T. Suzuki, K. Yoshida, and I. Tanihata, Physical Review Letters **84**, 5493 (2000).

[8] R. Kanungo, C. Nociforo, A. Prochazka, T. Aumann, D. Boutin, D. Cortina-Gil, B. Davids, M. Diakaki, F. Farinon, H. Geissel, *et al.*, Physical Review Letters **102**, 152501 (2009).

[9] C. Hoffman, T. Baumann, D. Bazin, J. Brown, G. Christian, D. Denby, P. DeYoung, J. Finck, N. Frank, J. Hinnefeld, S. Mosby, W. Peters, W. Rogers, A. Schiller, A. Spyrou, M. Scott, S. Tabor, M. Thoennessen, and P. Voss, Physics Letters B **672**, 17 (2009).

[10] K. Tshoo, Y. Satou, H. Bhang, S. Choi, T. Nakamura, Y. Kondo, S. Deguchi, Y. Kawada, N. Kobayashi, Y. Nakayama, *et al.*, Physical Review Letters **109**, 022501 (2012).

[11] Y. Kondo, N. Achouri, H. A. Falou, L. Atar, T. Aumann, H. Baba, K. Boretzky, C. Caesar, D. Calvet, H. Chae, *et al.*, Nature **620**, 965 (2023).

[12] M. Wang, W. Huang, F. Kondev, G. Audi, and S. Naimi, Chinese Physics C **45**, 030003 (2021).

[13] A. Mueller, D. Guillemaud-Mueller, J. Jacmart, E. Kashy, F. Pougheon, A. Richard, A. Staudt, H. Klapdor-Kleingrothaus, M. Lewitowicz, R. Anne, *et al.*, Nuclear Physics A **513**, 1 (1990).

[14] A. T. Reed, O. Tarasov, R. D. Page, D. Guillemaud-Mueller, Y. E. Penionzhkevich, R. G. Allatt, J. C. Angélique, R. Anne, C. Borcea, V. Burjan, W. N. Catford, Z. Dlouhý, C. Donzaud, S. Grévy, M. Lewitowicz, S. M. Lukyanov, F. M. Marqués, G. Martinez, A. C. Mueller, P. J. Nolan, J. Novák, N. A. Orr, F. Pougheon, P. H. Regan, M. G. Saint-Laurent, T. Siiskonen, E. Sokol, O. Sorlin, J. Suhonen, W. Trinder, and S. M. Vincent, Physical Review C **60**, 024311 (1999).

[15] Y. E. Penionzhkevich, Physics of Atomic Nuclei **64**, 1121 (2001).

[16] L. Cáceres, A. Lepailleur, O. Sorlin, M. Stanoiu, D. Sohler, Z. Dombradi, S. Bogner, B. Brown, H. Hergert, J. Holt, *et al.*, Physical Review C **92**, 014327 (2015).

[17] A. Stolz, T. Baumann, T. Ginter, D. Morrissey, M. Portillo, B. Sherrill, M. Steiner, and J. Stetson, Nuclear Instruments and Methods in Physics Research Section B: Beam Interactions with Materials and Atoms **241**, 858 (2005).

[18] D. Morrissey, B. Sherrill, M. Steiner, A. Stolz, and I. Wiedenhoever, Nuclear Instruments and Methods in Physics Research Section B: Beam Interactions with Materials and Atoms **204**, 90 (2003), 14th International Conference on Electromagnetic Isotope Separators and Techniques Related to their Applications.

[19] R. Yokoyama, M. Singh, R. Grzywacz, A. Keeler, T. King, J. Agramunt, N. Brewer, S. Go, J. Heideman, J. Liu, S. Nishimura, P. Parkhurst, V. Phong, M. Rajabali, B. Rasco, K. Rykaczewski, D. Stracener, J. Tain, A. Tolosa-Delgado, K. Vaigneur, and M. Wolińska-Cichocka, Nuclear Instruments and Methods in Physics Research Section A: Accelerators, Spectrometers, Detectors and Associated Equipment **937**, 93 (2019).

[20] W. Peters, S. Ilyushkin, M. Madurga, C. Matei, S. Paulauskas, R. Grzywacz, D. Bardayan, C. Brune, J. Allen, J. Allen, *et al.*, Nuclear Instruments and Methods in Physics Research Section A: Accelerators, Spectrometers, Detectors and Associated Equipment **836**, 122 (2016).

[21] S. Paulauskas, M. Madurga, R. Grzywacz, D. Miller, S. Padgett, and H. Tan, Nuclear Instruments and Methods in Physics Research Section A: Accelerators, Spectrometers, Detectors and Associated Equipment **737**, 22 (2014).

[22] C. J. Gross, T. Ginter, D. Shapira, W. Milner, J. McConnell, A. James, J. Johnson, J. Mas, P. Mantica, R. Auble, *et al.*, Nuclear Instruments and Methods in Physics Research Section A: Accelerators, Spectrometers, Detectors and Associated Equipment **450**, 12 (2000).

[23] M. S. Basunia and A. Chakraborty, Nuclear Data Sheets **186**, 2 (2022).

[24] S. Agostinelli, J. Allison, K. Amako, J. Apostolakis, H. Araujo, P. Arce, M. Asai, D. Axen, S. Banerjee, G. Barrand, F. Behner, L. Bellagamba, J. Boudreau, L. Broglia, A. Brunengo, H. Burkhardt, and S. C. et al., Nuclear Instruments and Methods in Physics Research Section A: Accelerators, Spectrometers, Detectors and Associated Equipment **506**, 250 (2003).

[25] J. Allison, K. Amako, J. Apostolakis, P. Arce, M. Asai, T. Aso, E. Bagli, A. Bagulya, S. Banerjee, G. Barrand, B. Beck, A. Bogdanov, D. Brandt, J. Brown, H. Burkhardt, P. Canal, D. Cano-Ott, and S. C. et al., Nuclear Instruments and Methods in Physics Research Section A: Accelerators, Spectrometers, Detectors and Associated Equipment **835**, 186 (2016).

[26] H. Ohm, W. Rudolph, and K.-L. Kratz, Nuclear Physics A **274**, 45 (1976).

[27] Z. Y. Xu, M. Madurga, R. Grzywacz, T. T. King, A. Algora, A. N. Andreyev, J. Benito, T. Berry, M. J. G. Borge, C. Costache, H. De Witte, A. Fijalkowska, L. M. Fraile, H. O. U. Fynbo, A. Gottardo, C. Halverson, L. J. Harkness-Brennan, J. Heideman, M. Huyse, A. Il-

lana, L. Janiak, D. S. Judson, A. Korgul, T. Kurtukian-Nieto, I. Lazarus, R. Lică, R. Lozeva, N. Marginean, R. Marginean, C. Mazzocchi, C. Mihai, R. E. Mihai, A. I. Morales, R. D. Page, J. Pakarinen, M. Piersa-Siłkowska, Z. Podolyák, P. Sarriguren, M. Singh, C. Sotty, M. Stepaniuk, O. Tengblad, A. Turturica, P. Van Duppen, V. Vedia, S. Viñals, N. Warr, R. Yokoyama, and C. X. Yuan, Physical Review C **108**, 014314 (2023).

[28] M. S. Basunia and A. Chakraborty, Nuclear Data Sheets **171**, 1 (2021).

[29] B. A. Brown and W. A. Richter, Physical Review C **74**, 034315 (2006).

[30] K. Tsukiyama, S. Bogner, and A. Schwenk, Physical Review Letters **106**, 222502 (2011).

[31] H. Hergert, S. Bogner, T. Morris, A. Schwenk, and K. Tsukiyama, Physics Reports **621**, 165 (2016).

[32] J. Noga, R. J. Bartlett, and M. Urban, Chemical Physics Letters **134**, 126 (1987).

[33] K. Hebeler, S. K. Bogner, R. J. Furnstahl, A. Nogga, and A. Schwenk, Physical Review Letters C **83**, 031301 (2011).

[34] J. D. Watts and R. J. Bartlett, Chemical Physics Letters **258**, 581 (1996).

[35] P. Gysbers, G. Hagen, J. D. Holt, G. R. Jansen, T. D. Morris, P. Navrátil, T. Papenbrock, S. Quaglioni, A. Schwenk, S. R. Stroberg, and K. A. Wendt, Nature Physics **15**, 428 (2019).

[36] J. Okołowicz, M. Płoszajczak, and I. Rotter, Physics Reports **374**, 271 (2003).

[37] C.-X. Yuan, Chinese Physics C **41**, 104102 (2017).

[38] J. Okołowicz, M. Płoszajczak, R. Charity, and L. Sobotka, Physical Review C **97**, 044303 (2018).